ACADEMIA ROMÂNĂ
Revue Roumaine de Chimie
http://web.icf.ro/rrch/

Rev. Roum. Chim.,
2020, *65*(5), 481-489
DOI: 10.33224/rrch.2020.65.5.08

THE EFFECT OF THE COMPOSITION OF THE ALLOY OF RuO_2 AND Pt NANOCRYSTALS ON INTERMEDIATE ADSORPTION DURING METHANOL OXIDATION

Milica SPASOJEVIĆ,[a,*] Lenka RIBIC-ZELENOVIĆ,[b] Miroslav SPASOJEVIĆ[b] and Tomislav TRIŠOVIĆ[c]

[a]Innovation Center of the Faculty of Chemistry, University of Belgrade, Belgrade, Serbia
[b]Joint Laboratory for Advanced Materials of the Serbian Academy of Science, Section for Amorphous Systems, Faculty of Technical Sciences, Čačak, University of Kragujevac, Čačak, Serbia
[c]Institute of Technical Sciences of the Serbian Academy of Science, Belgrade, Serbia

Received March 22, 2020

A catalytic coating composed of a mixture of RuO_2 and Pt nanocrystals was prepared by a thermal procedure on a titanium substrate and used for the electrochemical oxidation of methanol. The adsorption of the intermediate CO, formed by methanol oxidation on Pt nanocrystals, depended on potential and the coating composition. An increase in the RuO_2 content decreased the rate of methanol dehydrogenation and increased the rate of oxidation of the strongly bound intermediate CO_{ad}. This caused a decrease in the maximum coverage of Pt nanocrystals with CO_{ad} and a shift of the rapid linear drop in CO_{ad} coverage to more negative potentials.

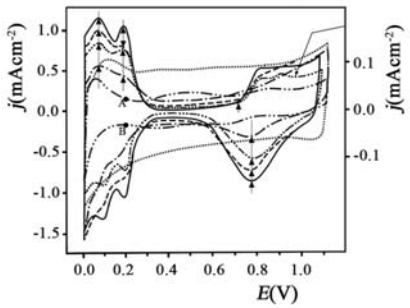

INTRODUCTION

The application of H_2 in fuel cells is difficult due to many obstacles such as high costs of miniaturized hydrogen containers, potential dangers during the use of hydrogen and possible hazards during its transport. Moreover, hydrogen has a low gas-phase energy density.[1] Therefore, the possible use of methanol in fuel cells has lately been the subject of many research groups. Methanol fuel cells are attractive alternatives for small portable applications.[2] Liquid methanol has high energy density. However, the electrochemical oxidation of methanol is slow and followed by the formation of intermediates such as CO_{ad}, COH_{ad} and HCOO.[3–8] These species will strongly adsorb on the surface of the most effective catalyst, *i.e.* Pt, thus blocking the surface for the oxidation of subsequent methanol molecules[3–6]. Therefore, platinum-based electrocatalysts, such as PtSn,[7] PtTi,[8,9] PtMn,[10,11] PtCo,[12–14] PtFe,[15,16] PtBi,[17,18] PtPb,[17,19] Pt_3Ni,[11,20] PtZn,[21–24] PtCu,[25–28] PtCuCo[29] and PtRu[2–6,29–44] are of great interest for fuel cell applications. Research groups have mostly focused on determining the effect of the content and morphology of nanoparticles on their catalytic activity towards the oxidation of methanol and other simple organic molecules. Also, it has been shown that the size of nanocrystals influenced the electronic structure and catalytic activity towards the electrooxidation of methanol[29, 45, 46].

In the past two decades, researchers have found that Pt, Ru catalysts showed the best catalytic properties in fuel cell applications.[3-6,29–44] The catalytic effect of Pt, Ru alloys was attributed to the bifunctional mechanism and the electronic

* Corresponding author: smilica84@gmail.com

effect. Catalysis was mostly caused by the bifunctional mechanism, where Ru atoms were able to form oxy species at substantially more negative potentials than Pt. These oxy species oxidized CO_{ad} intermediates, which were strongly adsorbed on adjacent Pt atoms, and thus discharged those Pt atoms for the adsorption and dehydrogenation of subsequent methanol molecules.[3–6,29–44] The electronic effect was the result of the d-band center shift of Pt in the Pt/Ru alloys, away from the Fermi level.[30, 34–37, 39] This caused weaker adsorption of the poisoning CO_{ad} species and therefore reduced the poisoning effect. Weakly bound intermediates were more rapidly oxidized by oxy species, plausibly OH_{ad}, which were adsorbed at adjacent Pt or Ru atoms.[30, 34–37, 39]

The aim of this research was to investigate the effect of potential and the composition of a mixture of RuO_2 and metallic Pt nanocrystals on the adsorption of intermediates, strongly bound to Pt nanocrystals, during the electrooxidation of methanol. Knowledge of the nature of this effect allows for the determination of parameters for the preparation of the alloy having an optimal composition and structure which provides maximum catalytic activity for methanol electrooxidation.

RESULTS AND DISCUSSION

Coatings composed of various amounts of nanocrystals of RuO_2 and metallic Pt were synthetized by a thermal procedure on a properly prepared titanium substrate. Six different coatings were made: 1) 100 mol% Pt, 2) 80 mol% Pt, 20 mol% RuO_2, 3) 60 mol% Pt, 40 mol% RuO_2, 4) 40 mol% Pt, 60 mol% RuO_2, 5) 20 mol% Pt, 80 mol% RuO_2, and 6) 100 mol% RuO_2. XRD analysis was used to determine the microstructural properties of the coatings. It was found that the coatings were composed of RuO_2 nanocrystals of rutile structure and nanocrystals of the FCC phase of metallic Pt.[47–51] The mean size of nanocrystals depended on the alloy composition. With increasing RuO_2 content in the alloy, the mean particle size of RuO_2 increased, whereas that of metallic Pt decreased[47] (Table 1).

The lattice of these thermally prepared nanocrystals of rutile RuO_2 and metallic Pt was slightly disordered in comparison to that of pure rutile RuO_2 and metallic platinum. This was a consequence of inclusion of small quantities of residual chlorine. Residual chlorine increased internal microstrains, causing a high density of chaotically distributed dislocations.[52–57]

Surface properties of the coatings were determined by analyzing the cyclic voltammograms recorded in the primary electrolyte.

The cyclic voltammograms of the thermally synthesized Pt coating and the pure Pt polycrystalline electrode were similar (Figure 1). The potentials of the maximum of hydrogen adsorption and desorption, the potentials of the reduction maximum and the beginning of Pt oxide formation at the electrode with more than 60 mol% Pt were comparable to those at polycrystalline Pt (see arrows in Figure 1). This indicated that the surface structure of the thermally formed Pt nanocrystals with the mean size of crystalline particles larger than 4 nm did not differ from that of polycrystalline Pt.[47] The current formed in a redox process on Ru atoms of the coating with less than 40 mol% Pt was relatively large. Therefore, it was impossible to distinguish it from the current assigned to Pt nanocrystals.

Table 1

Mean particle size of RuO_2 and metallic Pt as a function of coating composition

Coating composition	100 mol% Pt	80 mol% Pt, 20 mol% RuO_2		60 mol% Pt, 40 mol% RuO_2	
Particle	Pt	Pt	RuO_2	Pt	RuO_2
Mean particle size (nm)	22±1.5	9±1.0	16±1.5	4±0.8	19±1.5
Coating composition	40 mol% Pt, 60 mol% RuO_2		20 mol% Pt, 80mol% RuO_2		100 mol% RuO_2
Particle	Pt	RuO_2	Pt	RuO_2	RuO_2
Mean particle size (nm)	<3	27±1.6	<3	35±1.8	42±1.8

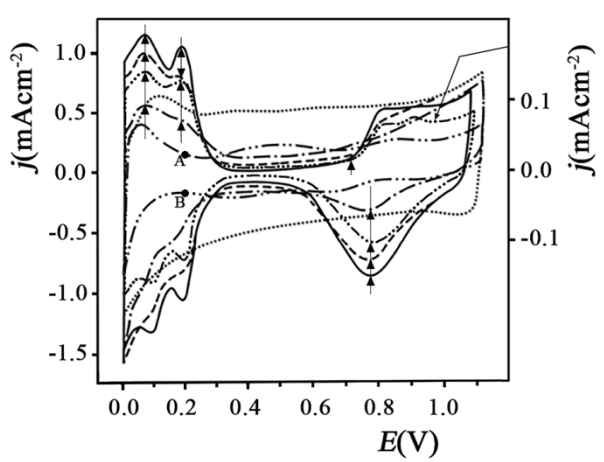

Fig. 1 – The cyclic voltammograms of the coatings: (—) 100 mol% Pt; (---) 80 mol% Pt, 20 mol% RuO_2; (•–•) 60 mol% Pt, 40 mol% RuO_2; (••••) 100 mol% RuO_2; (–•••) polycrystalline Pt; (••–) polycrystalline Ru. Sweep rate 100 mVs^{-1} (0.5 mol dm^{-3} H_2SO_4, t = 25°C).

The cyclic voltammograms of the coatings composed of either metallic Ru or RuO_2 showed that binding energies of oxy species to Ru atoms were different for these two electrodes. When metallic Ru was used, during the potential shift to the cathodic side, the oxy species were reduced until 0.2 V (Figure 1, point B). After reduction of the oxy species, the adsorption of hydrogen occurred. During the potential shift to the anodic side, hydrogen was desorbed until 0.2 V (Figure 1, point A). Subsequently, the oxy species were formed at more positive potentials (Figure 1). The same results were obtained by reflectance spectroscopy and ellipsometry.[58,59] However, the oxy species existed on Ru atoms of the RuO_2 coating at potentials more negative than 0.2 V.[58,59] The potential of oxy species formation on the RuO_2 coating could not be determined from the cyclic voltammograms due to the overlapping currents of hydrogen desorption and oxy species formation.

Methanol electrooxidation occurred as a multistage process. First, CH_3OH was gradually dehydrogenated on Pt atoms. This was followed by the formation of the strongly adsorbed intermediate CO_{ad}:[60–64]

$$CH_3OH + Pt \rightarrow Pt\text{-}CO_{ad} + 4H^+ + 4e^- \quad (1)$$

Then, the strongly bound intermediates were oxidized by the oxy species, plausibly OH_{ad}, formed on Pt or Ru atoms:[2-6,29-44,60-64]

$$Pt\text{-}CO_{ad} + Pt\text{-}OH \rightarrow 2Pt + CO_2 + H^+ + e^- \quad (2)$$

$$Pt\text{-}CO_{ad} + Ru\text{-}OH \rightarrow Pt + Ru + CO_2 + H^+ + e^- \quad (3)$$

Reactions (1)–(3) formed the main reaction pathway of methanol oxidation. Besides this main pathway, side reactions also occurred:[60–64]

$$Pt\text{-}CH_2OH_{ad} + OH_{ad} \rightarrow CH_2(OH)_2 + Pt \quad (4)$$

$$Pt\text{-}CHO_{ad} + OH_{ad} \rightarrow HCOOH + Pt \quad (5)$$

The products, $CH_2(OH)_2$ and HCOOH, were transported into a solution or oxidized at the electrode. However, the rates of reactions (4) and (5), and electrooxidation of $CH_2(OH)_2$ and HCOOH were negligible when compared to the rate of the main reaction pathway.

The degree of equilibrium coverage of Pt with the strongly adsorbed intermediates, CO_{ad}, at the specific methanol concentration and solution temperature, depended on both the free energy of intermediate CO_{ad} adsorption, $\Delta G(CO_{ad})$, and the ratio of the rate of methanol dehydrogenation, ν_d, to the rate of intermediate CO_{ad} oxidation, ν_{ox}.

Alloying Pt with Ru caused a decrease in $\Delta G(CO_{ad})$ and therefore in the degree of equilibrium coverage of Pt with the intermediates, CO_{ad}.[7, 8, 30, 34–37, 39] When $\Delta G(CO_{ad})$ was substantially less than zero and the ratio $\nu_d^{\theta}/\nu_{ox}^{\theta}$ considerably greater than 1, a large coverage degree of Pt was achieved $\theta(CO_{ad})$. When the rate of oxidation was essentially greater than the rate of dehydrogenation, the coverage degree, $\theta(CO_{ad})$, was almost zero. Rates of methanol dehydrogenation and CO_{ad} oxidation depended on both potential and the composition of the alloy consisting of Pt and RuO_2 nanocrystals. With increasing potential, the ratio $\nu_d^{\theta}/\nu_{ox}^{\theta}$ changed due to different dependences of ν_d^{θ} and ν_{ox}^{θ} rates on potential. The composition of the alloy consisting of Pt and RuO_2 nanocrystals had both direct and indirect effects on the rates of methanol dehydrogenation and CO_{ad} oxidation.

The direct influence was the result of the change in the size of the contact edge between RuO_2 and Pt nanocrystals, as well as of the variation in the number of available Pt atoms for methanol dehydrogenation. With increasing RuO_2 content, the contact edge initially increased and reached its maximum at the RuO_2 content of around 50 mol%.[48] Further increase in the RuO_2 content resulted in a decrease in the length of the contact edge. The increase in the size of the contact edge raised the number of adjacent pairs of Pt and Ru, and therefore, the rate of oxidation of the strongly bound intermediates CO_{ad} (reaction 3). However, the increase in the RuO_2 content decreased the number of surface Pt atoms and therefore the rate of methanol dehydrogenation.

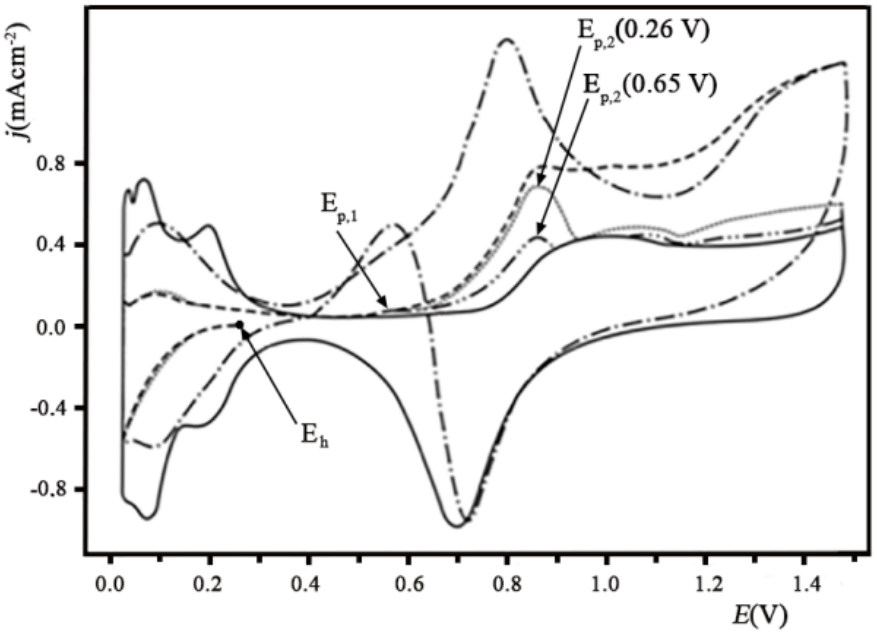

Fig. 2 – The cyclic voltammograms of the 100 mol% Pt electrode in:(—)- 0.5 mol dm^{-3} H_2SO_4; (–•–)- 0.5 mol dm^{-3} H_2SO_4 + 0.05 mol dm^{-3} CH_3OH; (----)- 0.5 mol dm^{-3} H_2SO_4 + 0.05 mol dm^{-3} CH_3OH, recorded after holding the electrode for 20 minutes at a potential of 0.26 V; (••••) and (–••–) recorded after holding the electrode for 20 minutes at a potential of 0.26 V and 0.65 V, respectively, in the solution 0.5 mol dm^{-3} H_2SO_4 + 0.05 mol dm^{-3} CH_3OH and after replacement of this solution with the basic electrolyte 0.5 mol dm^{-3} H_2SO_4. Sweep rate 166 mV s^{-1}, t = 25°C. (For clarity, only part of the curve (–••–) is presented.)

The indirect influence of the change in the RuO_2 content was a consequence of variations in the mean size of nanocrystals of Pt and RuO_2. The decrease in the mean size caused: a) an increase in the length of contact borders and therefore, in the rate of oxidation of the intermediates CO_{ad}, and b) a decrease in the number of assemblies that contained a sufficient number of Pt atoms suitable for complete dehydrogenation of methanol. When the composition of the coating was consistent and nanocrystals were larger than 4 nm, the number of assemblies at the Pt surface decreased linearly and slowly with decreasing size of nanocrystals. However, further decrease in the size of nanocrystals below 4 nm caused a rapid decline in the number of assemblies and thus in the rate of methanol dehydrogenation[45]. Therefore, in this paper, we investigated the effect of potential and the composition of the alloy of Pt and RuO_2 nanocrystals on the degree of coverage of platinum with the strongly bound intermediates CO_{ad}.

The degree of coverage of Pt nanocrystals with the strongly bound intermediates was determined in two ways. In the first procedure, known as „washing procedure",[49] after holding the electrodes for 10 s at a potential of 1.5 V, the potential was rapidly changed to the given value E_h. At this potential, the adsorption of organic species on Pt from the solution of specific composition occurred in time *t*. Thereafter, the solution with CH_3OH was replaced with the basic electrolyte and the cyclic voltammogram was recorded.

Two peaks, observed at the voltammograms (••••) and (–••–), are a consequence of the oxidation of the adsorbed intermediates strongly bound to Pt atoms. These particles were not desorbed during the "washing procedure". The first peak ($E_{p,1}$) was less pronounced and its maximum was at approximately 0.55 V, whereas the maximum of the other, more pronounced peak was at 0.85 V ($E_{p,2}$). The size of the second peak depended on the adsorption potential and the coverage degree, whereas the potentials of the maximum of both peaks were independent of these parameters. This indicated that two types of particles were adsorbed on Pt. The coverage degree of one type of particles was always low, whereas the coverage degree of the other type of particles depended on the adsorption potential and the methanol concentration in the solution[64]. Figure 2 shows that the peak $E_{p,2}$ (0.26V), obtained after holding the potential at 0.26 V, is substantially larger than peak $E_{p,2}$ (0.65V), recorded when the potential was held at 0.65 V. Additionally, the peaks $E_{p,1}$(0.26V) and $E_{p,1}$(0.65V) are small and approximately equal in size (see Figure 2). With

shifting the holding potential to more negative values, from 0.75 to 0.4 V, the size of the $E_{P,2}$ peak increases whereas the size of $E_{p,1}$ stays approximately the same. With this change in the holding potential, the degree of equilibrium coverage of Pt with CO_{ad} increases from 0.1 to 0.8 (Figure 6.). The dehydrogenation of adsorbed methanol resulted in the formation of $–CH_2OH$ particles, which were bound to one Pt atom.[60-64]

The particle =CHOH, formed in the second stage, required two adjacent Pt atoms for its adsorption.[60-64] In the third stage, a H atom, bound to carbon or oxygen, was detached. The detachment of hydrogen from carbon resulted in the formation of $\equiv$COH particles[60-64]. The adsorption of these particles required three adjacent free Pt atoms. By detaching hydrogen from oxygen, –CHO particles were formed.[60-64] These particles could adsorb on one free Pt atom. With increasing the coverage degree, the number of assemblies composed of three Pt atoms rapidly decreased, whereas the number of free Pt atoms declined linearly. Thus, the particles $\equiv$COH could only be formed at low coverage degrees, whereas –CHO could successfully be established at both low and high degrees of coverage.

After the potential drop from 1.5 V to $E < 0.4$ V, methanol molecules and intermediates were rapidly adsorbed on an electrode from the concentrated solutions of methanol. This resulted in a very small amount of assemblies composed of three adjacent free atoms. Therefore, in the cyclic voltammograms recorded in the concentrated methanol solutions, the first peak was not observed. In the diluted methanol solution, the time required for intermediate adsorption was longer. Therefore, by using these solutions, $\equiv$COH particles were formed on the surface of Pt. The number of these particles was low and increased by diluting the solution, which resulted in an increase in the size of the first peak.

The appearance of the first peak was the result of reactions (6) and (7):

$$\text{Pt-COH}_{ad} \rightarrow \text{Pt-CO}_{ad} + H^+ + e^- \quad (6)$$

$$\text{Pt-COH}_{ad} + \text{Pt-OH} \rightarrow 2\text{Pt} + CO_2 + 2H^+ + 2e^- \quad (7)$$

The cyclic voltammogram of the Pt electrode in the solution 0.5 mol dm^{-3} H_2SO_4 + 0.05 mol dm^{-3} CH_3OH, obtained after holding the potential for 20 minutes at 0.26 V, showed that the current of methanol oxidation did not exist before the oxidation of the strongly bound intermediates. This indicated that the equilibrium coverage of adsorbed intermediates was established in 20 minutes. However, the cyclic voltammograms obtained without the potential hold showed that, even at potentials more negative than the potential of the oxidation of adsorbed intermediates, the current of methanol oxidation emerged. This indicated that the equilibrium coverage of the electrode was not achieved and, adsorption and dehydrogenation of methanol occurred at those more negative potentials. In accordance with the first procedure, the „washing procedure", the degree of coverage, θ, (θ applies only to the surface Pt atoms) was determined using the equation: $\theta = Q_{CO}/2{}_SQ_H$, where Q_{CO} and ${}_SQ_H$ are the oxidation peak charge of adsorbed CO_{ad} and the desorption charge of hydrogen fully adsorbed on all Pt sites in the methanol – free electrolyte, respectively.

In the second procedure, the degree of coverage of the electrode with intermediates adsorbed only from the diluted solutions of methanol was determined. Adsorption was determined by holding the electrode for 10 s at a potential of 1.5 V. Thereafter, the potential was rapidly set to the given value *E*. At this potential, the adsorption of organic particles at Pt nanocrystals from diluted solutions in the time period *t* occurred. After the time period *t*, a cyclic voltammogram was recorded. At a relatively high sweep rate (166 mV s^{-1}) and at low concentrations of the solution (<0.05 mol dm^{-3} CH_3OH), the coverage degree did not change substantially, with the potential shift to the cathodic side from *E* to 0.0 V and to the anodic side from 0.0 to 0.4 V. The degree of coverage the electrode with organic particles was determined from the decrease in the current of hydrogen desorption (Figure 3). The calculation was performed using the equation: $\theta = ({}_SQ_H - Q_H)/{}_SQ_H$, where Q_H and ${}_SQ_H$ are the desorption charge of hydrogen in the methanol electrolyte and the desorption charge of hydrogen fully adsorbed on all Pt sites in the methanol – free electrolyte, respectively.

The coverage degrees determined after holding the electrode at potentials $E > 0.1$ V longer than 20 minutes were similar (±2% difference). Sungho Park *et al.*[64] have discovered that the second procedure provided better results. Therefore, only θ values obtained by this procedure are presented in this paper. In order to obtain more precise values of the degree of coverage, the diluted solution of methanol was used.

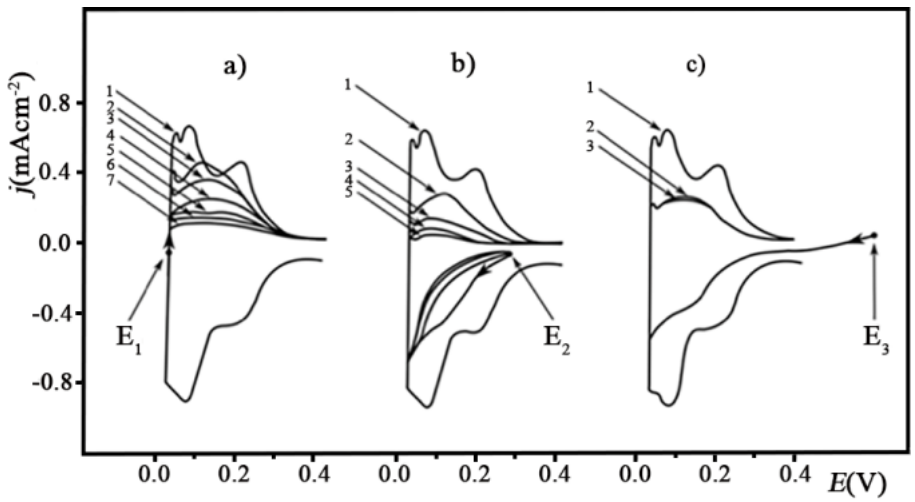

Fig. 3 – The cyclic voltammograms of 100 mol% Pt in 0.5 mol dm^{-3} H_2SO_4 + 0.05 mol dm^{-3} CH_3OH, recorded after holding at potential: a) E_1 = 0.010 V; b) E_2 = 0.255 V; c) E_3 = 0.580 V; 1 – basic curve (without CH_3OH); 2 – 0.5 min; 3 – 2 min; 4 – 8 min; 5 – 20 min; 6 – 40 min; 7 – 80 min. Sweep rate 166 mVs^{-1}, t=25°C.

The dependence of the degree of coverage, θ, of the thermally synthesized Pt coatings with intermediates on potential and time of adsorption is presented in Figure 4. The rate of adsorption and thus, the time required to reach equilibrium (maximum) coverage depended on potential, as seen in Figure 4. In the double-layer region, equilibrium coverage was rapidly established (t < 2 min). Adsorption was considerably slower in the hydrogen region. In the potential region from 0.15 to 0.45 V, equilibrium coverage was established in approximately 20 minutes. At potentials lower than 0.15 V, with a further decrease in potential, the rate of adsorption was rapidly decreased. This rapid decrease was caused by 1) an increase in the degree of coverage of Pt with adsorbed hydrogen, θ_H, 2) an increase in the strength of bond between hydrogen and platinum, and 3) a decrease in the rate of charge exchange during methanol dehydrogenation.

In the potential region from 0.0 V to 0.5 V, the equilibrium coverage degree was independent of potential. In this potential region, the rate of methanol dehydrogenation was considerably higher than the rate of oxidation of strongly bound intermediates. At potentials more positive than 0.75 V, the rate of intermediate oxidation was substantially greater than the rate of methanol dehydrogenation. Therefore, Pt surface was completely free of strongly bound intermediates at the above mentioned potentials. A linear drop of the coverage degree started at potentials where the rate of methanol dehydrogenation was equivalent to the rate of CO_{ad} oxidation. Further increase in potential raised the rate of CO_{ad} oxidation more than the rate of CH_3OH dehydrogenation, thus lowering the degree of coverage. This decrease of the coverage degree simultaneously declined the rate of oxidation and elevated the rate of dehydrogenation until these two rates became even again. This process continued as long as the adsorbed particles CO_{ad} were present on the surface.

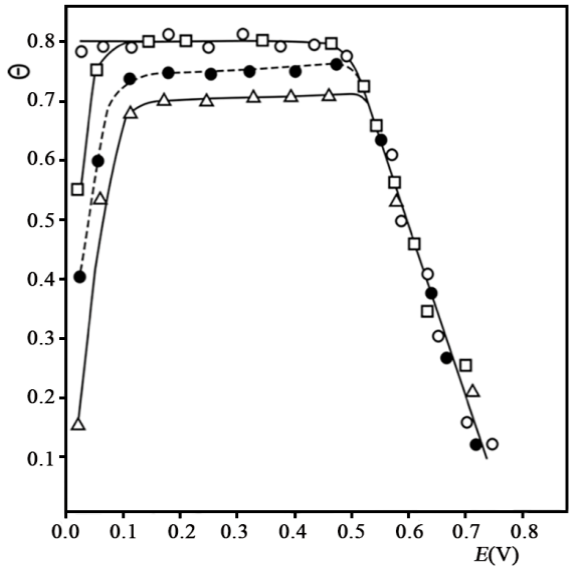

Fig. 4 – The degree of coverage of 100 mol% Pt with intermediates as a function of potential and adsorption time: △ – 2 min; ● – 8 min; □ – 20 min; ○ – 80 min (equilibrium coverage). (0.5 mol dm^{-3} H_2SO_4 + 0.05 mol dm^{-3} CH_3OH; t = 25°C).

As previously discussed, with increasing content of RuO_2 in the alloy consisting of Pt and RuO_2 nanocrystals, the rate of methanol dehydrogenation decreased, whereas the rate of

CO_{ad} oxidation increased, which resulted in a shift of the linear drop in the coverage degree to more negative potentials. This was corroborated by the experimental results presented in Figures 5 and 6.

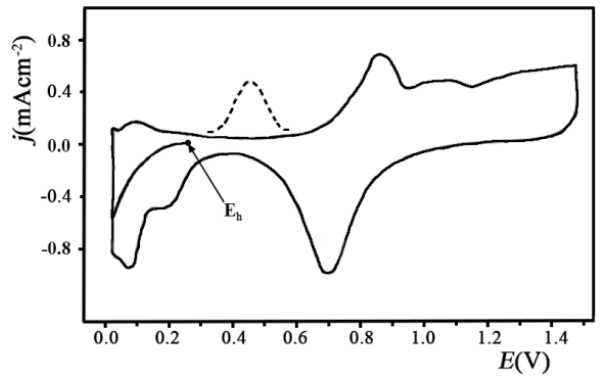

Fig. 5 – The first cyclic voltammograms of: (──) 100 mol % Pt and (- - -) 60 mol% Pt, 40 mol% RuO_2 (for clarity, only part of the curve (- - -) is presented) recorded after holding the electrodes for 20 minutes at 0.26V, in the solution 0.5 mol dm^{-3} H_2SO_4 + 0.05 mol dm^{-3} CH_3OH and after replacement of this solution with the basic electrolyte 0.5 mol dm^{-3} H_2S0_4. Sweep rate 166 mVs^{-1}, t = 25°C.

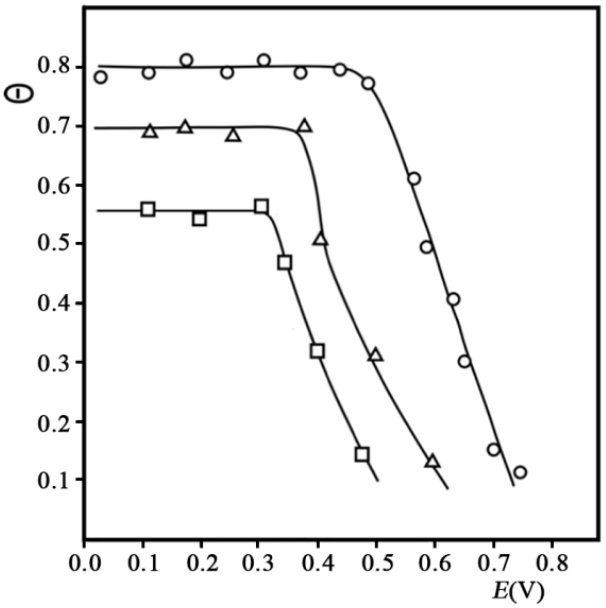

Fig. 6 – The degree of equilibrium coverage of the coatings composed of: ○ – 100 mol% Pt; △ – 80 mol% Pt, 20 mol% RuO_2; □ – 60 mol% Pt, 40 mol% RuO_2 with the intermediate CO_{ad} as a function of potential (0.5 mol dm^{-3} H_2SO_4 + 0.05 mol dm^{-3} CH_3OH; t = 25°C) (θ applies only to surface Pt atoms).

Figure 6 shows that the maximum coverage degree of Pt nanocrystals declined with increasing RuO_2 content. This was a consequence of the decrease in the ratio of the total number of assemblies of adjacent free Pt atoms to the total number of surface Pt atoms (n_s/n_a). With increasing content of RuO_2, the mean size of Pt nanocrystals decreased as did the probability of finding two or more adjacent terrace Pt atoms on smaller nanoparticles[45]. When the composition of the alloy was kept consistent, as the size of Pt nanocrystals decreased to 4 mm, the number of assemblies of two or more free terrace Pt atoms decreased slowly and linearly. However, with a further decrease in the size of Pt nanocrystals below 4 nm, the number of assembles as well as the rate rapidly declined.

The obtained results showed that 1) the alloy composed of Pt and RuO_2 nanocrystals catalyzed the CH_3OH oxidation reaction; 2) maximum catalytic effect was achieved when the mean size of Pt nanocrystals was around 4 nm; and 3) the optimal composition of the alloy depended on potential and, at more positive potentials, the RuO_2 content in the optimal alloy was lower.

EXPERIMENTAL

A titanium substrate, in the shape of plates with a surface area of 3.0 cm^2, was activated for the electrochemical oxidation of methanol by the thermal formation of a film of RuO_2 and metallic Pt. The solutions H_2PtCl_6 and $RuCl_3$ (Johnson and Matthey) in 2-propanol at a concentration of 10 mg cm^{-3} based on the pure metals were spread over the titanium plates. By adjusting the ratio H_2PtCl_6:$RuCl_3$ in the solution, the coatings of desired composition were obtained. Following the evaporation of the solvent, the electrodes were heated for 5 minutes at 500°C in the air atmosphere. The procedure was repeated five times until the coating depth of 1.2 mgm^{-2} based on the pure metals was reached. After spreading of the last layer, the electrodes were heated for 45 minutes at 500°C.

A Phillips PW1730 diffractometer equipped with a PW 1050 vertical goniometer and a static non-rotating sample carrier was used for X-ray diffraction analyses. This had a 35 kV, 20 mA power supply for copper excitation, and an AMR graphite monochromator. Phases were identified by reference to ASTM tables.

The electrochemical measurements were performed using the usual electrical set-up consisting of a potentiostat equipped with a programmer (Potentiostat-Galvanostat model 173, EGG Princeton, Applied Research, Princeton, USA), an x-y recorder (Hewlett Packard 7035 B) and a digital voltmeter (Pros´Kit 03-9303 C). The experiments were conducted in a standard electrochemical cell containing a separate compartment for a saturated mercury sulfate electrode and a Luggin capillary. The counter electrode was a flat platinum mesh with a geometric surface area of 16 cm^2 (4 x 4 cm) placed parallel to the working electrode. The cell was placed in the thermostat. The operating temperature was 25±0.5°C. The solutions were made from p.a. chemicals (Merc) and demineralized water. Prior to the electrochemical measurements, oxygen was removed from the solution by introducing nitrogen, which was purified beforehand by passing over molecular sieves and copper shavings. All potentials were expressed relative to the standard hydrogen electrode.

CONCLUSIONS

A catalytic coating was prepared by a thermal procedure on a titanium substrate and used in the electrooxidation of methanol. This coating was an alloy composed of RuO_2 nanocrystals of rutile structure and metallic platinum. It was found that, during methanol oxidation, the adsorption of intermediates, mostly CO_{ad}, depended on potential and the coating composition. The maximum coverage of Pt nanocrystals did not change substantially up to the potential at which intensive oxidation of CO_{ad} with oxy species formed at adjacent Pt and Ru atoms was initiated. Further increase of potential resulted in a linear decrease of the coverage degree to a negligibly small value. RuO_2 could directly and indirectly influence the coverage degree. The direct effect of the increase in the RuO_2 content was evidenced by an increase in the length of contact edges between nanocrystals of RuO_2 and Pt, and thus, in the number of adjacent Pt and Ru atoms. This caused an increase in the rate of oxidation of the CO_{ad} particles, adsorbed on Pt atoms, with the OH_{ad} particles, bound to adjacent Ru atoms. Simultaneously, with increasing RuO_2 content, the number of assemblies of adjacent Pt atoms required for methanol dehydrogenation decreased. The indirect effect of the increase in the RuO_2 content is a consequence of decline in the mean size of nanocrystals. This caused an increase in the size of contact edges and thus, in the rate of CO_{ad} oxidation, as well as a decrease in the number of assemblies of adjacent Pt atoms, and therefore in the rate of dehydrogenation. The direct and indirect effects related to the increase in the RuO_2 content resulted in a decrease in the equilibrium coverage and a shift of the linear drop in the coverage degree to more negative potentials.

Acknowledgements. This work was supported by the Ministry of Education and Science of the Republic of Serbia through Project Ref. No. 172 057.

REFERENCES

1. X. Yu and P. G. Pickup, *J. Power Sources,* **2008**, *182*, 124.
2. C. Rice, S. Ha, R.I. Masel, P. Waszczuk, A. Wieckowski and T. Barnard, *J. Power Sources,* **2002**, *111*, 83.
3. H. Liu, C. Song, L. Zhang, J. Zhang, H. Wang and D. P. Wilkinson, *J. Power Sources,* **2006**, *155*, 95.
4. X. Zhao, M. Yin, L. Ma, L. Liang, C. Liu, J. Liao, T. Lu and W. Xing, *Energy Environ. Sci.,* **2011**, *4*, 2736.
5. N. Kakati, J. Maiti, S. H. Lee, S. H. Jee, B. Viswanathan and Y. S. Yoon, *Chem. Rev.,* **2014**, *114,* 12397.
6. A. Heinzel and V. M. Barragán, *J. Power Sources,* **1999**, *84,* 70.
7. D. Y. DeSario and F. J. DiSalvo, *Chem. Mater.,* **2014**, *26,* 2750.
8. H. Abe, F. Matsumoto, L. R. Alden, S. C. Warren, H. D. Abruña and F. J. DiSalvo*, J. Am. Chem. Soc.,* **2008**, *130,* 5452.
9. Z. Cui, H. Chen, M. Zhao, D. Marshall, Y. Yu, H. Abruña and F. J. DiSalvo, *J. Am. Chem. Soc.*, **2014**, *136*, 10206.
10. Y. Kang and C. B. Murray, *J. Am. Chem. Soc.,* **2010**, *132*, 7568.
11. T. Ghosh, B. M. Leonard, Q. Zhou and F. J. DiSalvo, *Chem. Mater.,* **2010**, *22*, 2190.
12. H. Yang, J. Zhang, K. Sun, S. Zou and J. Fang, *Angew. Chem. Int. Ed.,* **2010**, *49*, 6848.
13. L. Liu, E. Pippel, R. Scholz and U. Gösele, *Nano Lett.,* **2009**, *9*, 4352.
14. D. Wang, H. L. Xin, R. Hovden, H. Wang, Y. Yu, D. A. Muller, F. J. DiSalvo and H. D. Abruna, *Nat. Mater.,* **2013**, *12*, 81.
15. W. Chen, J. Kim, S. Sun and S. Chen, *Langmuir*, **2007**, *23*, 11303.
16. D. Y. Wang, H. L. Chou, Y. C. Lin, F. J. Lai, C. H. Chen, J. F. Lee, B. J. Hwang and C. C. Chen, *J. Am. Chem. Soc.,* **2012**, *134,* 10011.
17. E. Casado-Rivera, D. J. Volpe, L. Alden, C. Lind, C. Downie, T. Vázquez-Alvarez, A. C. D. Angelo, F. J. DiSalvo and H. D. Abruña, *J. Am. Chem. Soc.,* **2004**, *126,* 4043.
18. X. Ji, K. T. Lee, R. Holden, L. Zhang, J. Zhang, G. A. Botton, M. Couillard and L. F. Nazar, *Nat. Chem.,* **2010**, *2*, 286 (2010).
19. F. Matsumoto, C. Roychowdhury, F. J. DiSalvo and H. D. Abruña, *J. Electrochem. Soc.,* **2008,** *155*, B148.
20. V. R. Stamenkovic, B. Fowler, B. S. Mun, G. Wang, P. N. Ross, C. A. Lucas and N. M. Marković, *Science,* **2007**, *315,* 493.
21. A. Miura, H. Wang, B. M. Leonard, H. D. Abruña and F. J. DiSalvo, *Chem. Mater.,* **2009**, *21*, 2661.
22. Y. Kang, J. B. Pyo, X. Ye, T. R. Gordon and C. B. Murray, *ACS Nano,* **2012**, *6*, 5642.
23. J. M. Gregoire, M. Kostylev, M. E. Tague, P. F. Mutolo, R. B. van Dover, F. J. DiSalvo and H. D. Abruña, *J. Electrochem. Soc.,* **2009**, *156,* B160.
24. Q. Chen, J. Zhang, Y. Jia, Z. Jiang, Z. Xie and L. Zheng, *Nanoscale,* **2014**, *6,* 7019.
25. D. Xu, Z. P. Liu, H. Z. Yang, Q. S. Liu, J. Zhang, J. Y. Fang, S. Z. Zou and K. Sun, *Angew. Chem., Int. Ed.,* **2009**, *48*, 4217.
26. B. Y. Xia, H. B. Wu, X. Wang and X. W. Lou, *J. Am. Chem. Soc.*, **2012**, *134*, 13934.
27. X. Sun, K. Jiang, N. Zhang, S. Guo and X. Huang, *ACS Nano,* **2015**, *9,* 7634.
28. F. Saleem, Z. Zhang, B. Xu, X. Xu, P. He and X. Wang, *J. Am. Chem. Soc.,* **2013**, *135,* 18304.
29. Z. Xia, P. Zhang, G. Feng, D. Xia and J. Zhang, *Adv. Mater. Interfaces,* **2018***, 1800297,* 1.
30. M. Wakisaka, S. Mitsui, Y. Hirose, K. Kawashima, H. Uchida and M. Watanabe, *J. Phys. Chem. B,* **2006***, 110,* 23489 .
31. H. A. Gasteiger, N. M. Markovic and P. N. Ross Jr, *J. Phys. Chem.,* **1995**, *99,* 8945.

32. B. N. Grgur, G. Zhuang, N. M. Markovic and P. N. Ross, *J. Phys. Chem.,* **1997**, *B 101*, 3910.
33. H. A. Gasteiger, N. Markovic, P. N. Ross Jr. and E. J. Cairns, *J. Phys. Chem.,* **1994**, *98,* 617.
34. M. A. Rigsby, W. P. Zhou, A. Lewera, H. T. Duong, P. S. Bagus, W. Jaegermann, R. Hunger and A. Wieckowski, *J. Phys. Chem.,* **2008***, C 112,* 15595.
35. H. Ataee-Esfahani, J. Liu, M. Hu, N. Miyamoto, S. Tominaka, K. C. W. Wu and Y. Yamauchi, *Small,* **2013**, *9*, 1047.
36. T. R. Garrick, W. Diao, J. M. Tengco, E. A. Stach, S. D. Senanayake, D. A. Chen, J. R. Monnier and J. W. Weidner, *Electrochim. Acta,* **2016**, *195*, 106.
37. M. Tian, S. Shi, Y. Shen and H. Yin, *Electrochim. Acta,* **2019**, *293,* 390.
38. S. Lu, K. Eid, D. Ge, J. Guo, L. Wang, H. Wang and H. Gu, *Nanoscale,* **2017**, *9*, 1033.
39. L. Feng, K. Li, J. Chang, C. Liu and W. Xing, *Nano Energy,* **2015**, *15*, 462.
40. C. Feng, T. Takeuchi, M. A. Abdelkareem, T. Tsujiguchi and N. Nakagawa, *J. Power Sources,* **2013**, *242,* 57.
41. L. Guo, S. Chen, L. Li and Z. Wei, *J. Power Sources,* **2014**, *247,* 360.
42. L. La-Torre-Riveros, R. Guzman-Blas, A. E. Méndez-Torres, M. Prelas, D. A. Tryk and C. R Cabrera, *ACS Appl. Mater. Interfaces,* **2012**, *4,* 1134.
43. Y. Cheng, C. Xu, P. K. Shen and S. P. Jiang, *Appl. Catal. B: Environ.,* **2014**, *158-159*, 140.
44. C. Nethravathi, E. A. Anumol, M. Rajamathi and N. Ravishankar, *Nanoscale,* **2011,** *3,* 569.
45. X. Huang, Z. Zhao, J. Fan, Y. Tan and N. Zheng, *J. Am. Chem. Soc.,* **2011**, *133,* 4718.
46. H. Wang, H. Y. Jeong, M. Imura, L. Wang, L. Radhakrishnan, N. Fujita, T. Castle, O. Terasaki and Y. Yamauchi, *J. Am. Chem. Soc.,* **2011**, *133,* 14526.
47. Milica Spasojevic, L. Ribic-Zelenovic, M. Spasojevic, *Russ J Electrochem, 56*, **2020**.
48 M. Spasojevic, L. Ribic-Zelenovic, Milica Spasojevic, T. Trisovic, *Russ. J. Electrochem.,* **2019***, 1350,* 55. 49 Milica Spasojevic, M. Spasojevic, L. Ribic-Zelenovic, *Monatsh. Chem.,* **2020**, *33,* 151.
50. Ch. Commnellis and G. P. Vercesi, *J. Appl. Electrochem*., **1991,**21,136.
51. L. P. R. Profeti, D. Profeti, P. Olivi*, Int. J. Hydrogen Energy*, **2009,**34, 2747.
52. Yu. E. Roginskaya, V. I. Bystrov and D. M. Shub, *Zh.Neorg. Khim*., **1977,**22,201.
53. J. Augustynski, L. Balsenc and J. Hinden, *J.Electrochem. So*c.,**1978,**125,1093.
54. G. Lodi, C.Deasnudies, S. Ardizzone, E.Siviery and S. Trasatti, *Surf. Technol*.,**1981,**14,335.
55. M. D. Spasojević, N. V. Krstajić, and M. M. Jakšić, *J. Mol. Catal.,* **1987**, *40,* 311.
56. M. Spasojevic, L. Ribic-Zelenovic, P. Spasojevic, *Ceram. Int.,* **2012**, *38,* 5827.
57. M. Spasojevic, N. Krstajic, P. Spasojevic, L. Ribic-Zelenovic, *Chem. Eng. Res. Des.,* **2015**, *93*, 591.
58. S. Hadzi-Jordanov, H. Angerstein-Kozlovska, M. Vukovic and B, E.Conway*, J. Phys. Chem*., **1977,** 81, 2271.
59. E.Ticanelli, J.G.Beery, M.T.Paffett and S. Gottesfeld, *J. Electroanal. Chem*.,**1989,** 258, 61.
60. O.A. Peetrii*, Russ. J. Electrochem*.**2019,** 55, 1.
61. S. V.Bagotzky, B. Yu. Vassiliev, and A. O. Khozova, *J. Electroanal. Chem*., **1977,** 81, 229.
62. L. J. Cohen, J. D. Volpe and D. H. Abruna, *Phys. Chem*., **2007,** 7,49.
63. M.H.T. Housmans, H.A.Wanders, M.T.M. Kopez, *J. Phys. Chem*. B. **2006,** 110, 10021**.**
64. Sungho Park, Yong Xie, and Michael J. Weaver, *Langmuir,* **2002,** 18, 5792.